

NONLINEAR PROPERTIES OF GATED GRAPHENE IN A STRONG ELECTROMAGNETIC FIELD

A.A. Avetisyan,^{1,*} A. P. Djotyan,^{1,†} and K. Mouloupoulos^{2,‡}

¹*Department of Physics, Yerevan State University,
1 A. Manoogian, 0025 Yerevan, Armenia*

²*Department of Physics, University of Cyprus,
P.O. Box 20537, 1678 Nicosia, Cyprus*

(Dated: October 4, 2018)

Abstract

We develop a microscopic theory of a strong electromagnetic field interaction with gated bilayer graphene. Quantum kinetic equations for density matrix are obtained using a tight binding approach within second quantized Hamiltonian in an intense laser field. We show that adiabatically changing the gate potentials with time may produce (at resonant photon energy) a full inversion of the electron population with high density between valence and conduction bands. In the linear regime, excitonic absorption of an electromagnetic radiation in a graphene monolayer with opened energy gap is also studied.

PACS numbers: 78.67.Wj, 71.35.Cc, 42.50.Hz, 73.50.Fq

*Electronic address: artakav@ysu.am

†Electronic address: adjotyan@ysu.am

‡Electronic address: cos@ucy.ac.cy

I. INTRODUCTION

Graphene, a two-dimensional (2D) crystal of carbon atoms packed in hexagonal lattice, has attracted great interest last years due to its exotic electronic properties [1, 2]. The charge carriers in graphene are massless Dirac fermions with effective "velocity of light" $v_F = 10^6 m/s$, that by two orders is smaller than the speed of light in vacuum.

The deep connection between the electronic properties of graphene and certain theories in particle physics makes graphene a testbed for many ideas in basic science. Besides the well-known electronic properties, such as ballistic electron transport [1–3] quantum Hall effect [4] tunable band gap [5, 6] graphene also shows very interesting optical properties [7]. Ultrathin graphite films with excellent mechanical quality and fascinating energy spectrum are very promising, e.g. for nanoelectronics [8] and as transparent conducting layers [9] which are important, e.g. for displays and solar cells.

Graphene has been extensively considered as a promising material for nonlinear optical applications [10]. In particular, the nonlinear quantum electrodynamics effects can be observed in graphene already for fields available in the laboratory [11]. In Ref. 10 the nonlinear optical response of electron dynamics in monolayer graphene to an intense light pulse was investigated. The study of the nonlinear electromagnetic effects in graphene has so far mainly focused on monolayer graphene. Meanwhile, there is growing interest in bilayer and trilayer graphene systems, where the electronic band structures are richer than in monolayer and can be easily manipulated by the application of external fields. Theoretical and experimental investigations have shown that a perpendicular electric field (created by gates) applied to a graphene bilayer modifies its band structure near the K point and may open an energy gap [12] in the electronic spectrum. Magnetotransport [12] and spectroscopic [6] measurements showed that the induced gap between the conduction and valence bands could be tuned between zero and midinfrared energies. This makes bilayer graphene the only known semiconductor with a tunable energy gap, and may open the way for developing photodetectors and lasers tunable by an electric field.

The magnitude of the gap also strongly depends on the number of graphene layers and its stacking order [13–15]. A desirable band structure for multilayer graphene systems, that can be useful for different purposes of nano- and optoelectronics, can be theoretically found (and suggested for an experimental realization) e.g. by a corresponding choice of the layer

number in a graphene system. Multilayer graphene systems exhibit rich novel phenomena at low charge densities owing to enhanced electronic interactions [15]. In [13, 14] we studied theoretically electric field induced band gap of graphene multilayers with different ways of stacking between consecutive graphene planes. Using a positively charged top and a negatively charged back gate it is possible to control independently the density of electrons on the graphene layers (correspondingly the band gap) and the Fermi energy of multilayer graphene systems.

Optical measurement techniques are widely adopted to experimentally investigate electronic properties of graphene multilayers. To determine the number of layers, as well as the stacking structure, Raman spectroscopy was used in [16, 17]. Infrared spectroscopy is also applied to probe the low-energy band structure. The dependence of the infrared optical absorption on the stacking sequence has been observed in recent experiments [18].

It is therefore of high relevance and of great interest to theoretically study nonlinear optical properties of multilayer graphene systems with opened energy gap between valence and conduction bands.

In the present work we develop a microscopic theory of a strong electromagnetic field interaction with bilayer graphene with an energy gap opened by external gates. We study the nonlinear response of bilayer graphene, when one-photon interband excitation regime is induced by an intense coherent radiation. We show that at resonant photon energy, close to the energy gap, and adiabatically changing the gate potentials with time, one can produce full inversion of the electron population with high density between the valence and conduction bands.

The coherent optical response of multilayer graphene systems to an intense laser radiation field may reveal many particle correlation effects. Excitons are expected to modify strongly the optical response. In monolayer graphene, since there is no energy gap, the Coulomb problem has no true bound states, but resonances [19]. A signature of the presence of the excitonic resonances was observed in its optical properties [20]. The optical response of graphene with an opened energy gap between the conduction and valence bands is dominated by bound excitons [21].

In this work, we also study the excitonic absorption of a monolayer graphene with an opened energy gap. A substantial band gap in monolayer graphene can be induced in several ways, e.g., by coupling to substrates, electrical biasing, or nanostructuring [2].

The plan of the paper is as follows. Section II presents an outline of the underlying theory and describes the laser interaction with a gated graphene system. The evolution equations for the single-particle density matrix in the presence of Coulomb interaction are obtained in Section III. Excitonic absorption in monolayer graphene is investigated in Section IV. Section V contains our numerical results together with a discussion of essential physical points. Section VI presents our main conclusions.

II. LASER INTERACTION WITH GATED BILAYER GRAPHENE

We consider here the interaction of a strong electromagnetic wave with bilayer graphene. A perpendicular electric field created by top and back gates [13] opens an energy gap in multilayer graphene. We assume that the laser pulse propagates in the perpendicular direction to graphene plane (XY) and the electric field $\mathbf{E}(t)$ of pulse lies in the graphene plane.

The Hamiltonian in the second quantization formalism has the form

$$\hat{H} = \int \hat{\Psi}^\dagger H_s \hat{\Psi} d\mathbf{r} \quad (1)$$

The Hamiltonian H_s for bilayer, in the vicinity of the K point, for energies $\varepsilon \ll \gamma_1$ (with $\gamma_1 = 377\text{meV}$ being the vertical interlayer hopping parameter) can be written as (here we omit the real spin number):

$$\hat{H}_s = \hat{H}_0 + \hat{H}_d, \quad (2)$$

$$\hat{H}_0 = \begin{pmatrix} -\frac{U}{2} & -\frac{\hbar^2}{2m}(k_x - ik_y)^2 + v_3\hbar(k_x + ik_y) \\ -\frac{\hbar^2}{2m}(k_x + ik_y)^2 + v_3\hbar(k_x - ik_y) & \frac{U}{2} \end{pmatrix}, \quad (3)$$

$$\hat{H}_d = \begin{pmatrix} \mathbf{e}\mathbf{r} \cdot \mathbf{E}(t) & 0 \\ 0 & \mathbf{e}\mathbf{r} \cdot \mathbf{E}(t) \end{pmatrix}. \quad (4)$$

The first term in Eq. (2) corresponds to bilayer graphene in the field of perpendicular electric field: U is the gap introduced by the perpendicular electric field, and the second term is the interaction Hamiltonian between a laser field and bilayer graphene; $v_3 \approx v_F/8$ is the effective velocity $v_3 = \sqrt{3}\gamma_3 a/2\hbar$ where γ_3 describes the interaction between B atoms in the

neighbouring layers, and a is the lattice constant. The account of this interaction leads to the so called triangular warping effect of the bands [13]. The Fermi velocity $v_F = \sqrt{3}\gamma_0 a/2\hbar \simeq 10^6 m/s$ and tight-binding parameter γ_0 describes the interaction between A and B atoms in the same layer, $\mathbf{p} = \hbar\mathbf{k}$ is the electron momentum and $\mathbf{k} = \{k_x, k_y\}$.

We expand the fermionic field operator over the free wave function $\psi_\sigma(\mathbf{k})$ of bilayer graphene

$$\Psi(\mathbf{r}, t) = \sum_{\sigma\mathbf{k}} \hat{a}_{\mathbf{k},\sigma}(t) \Psi_\sigma(\mathbf{k}) e^{i\mathbf{k}\mathbf{r}} \quad (5)$$

where the annihilation operator $\hat{a}_{\mathbf{p},\sigma}(t)$ is associated with positive and negative energy solutions $\sigma = \pm 1$. Introducing $\vartheta(\mathbf{k}) = \arctan(k_y/k_x)$, $k_x + ik_y = k e^{i\vartheta}$ the expression for energy spectrum of bilayer graphene can be brought to the form

$$\mathcal{E}_{\mathbf{k}\sigma} = \sigma \sqrt{\frac{U^2}{4} + (v_3 \hbar k)^2 - \frac{v_3 \hbar^3 k^3}{m} \cos 3\vartheta + \left(\frac{\hbar^2 k^2}{2m}\right)^2} \quad (6)$$

The free solutions in bilayer graphene $\psi_\sigma(\mathbf{k})$ have the following form

$$\psi_\sigma(\mathbf{k}) = \sqrt{\frac{\mathcal{E}_{\mathbf{k}\sigma} + U/2}{2\mathcal{E}_{\mathbf{k}\sigma}}} \begin{pmatrix} 1 \\ \frac{1}{\mathcal{E}_{\mathbf{k}\sigma} + U/2} \Upsilon(k, \vartheta) \end{pmatrix}, \quad (7)$$

where

$$\Upsilon(k, \vartheta) = -\frac{\hbar^2 k^2}{2m} e^{i2\vartheta} + v_3 \hbar k e^{-i\vartheta}. \quad (8)$$

Taking into account Eqs. (1)-(5), the second quantized Hamiltonian for the single-particle part can be expressed as

$$\hat{H} = \sum_{\mathbf{k},\sigma} \mathcal{E}_{\mathbf{k}\sigma} \hat{a}_{\mathbf{k}\sigma}^\dagger \hat{a}_{\mathbf{k}\sigma} + e\mathbf{E}(t) \sum_{\mathbf{k},\sigma} \sum_{\mathbf{k}',\sigma'} \mathbf{D}_{\sigma\sigma'}(\mathbf{k}, \mathbf{k}') \hat{a}_{\mathbf{k}\sigma}^\dagger \hat{a}_{\mathbf{k}'\sigma'}, \quad (9)$$

For the dipole matrix element for transition between the valence and conduction bands

$$d_{\sigma\sigma'}(\mathbf{k}, \mathbf{k}') = ie \mathbf{D}_{\sigma\sigma'}(\mathbf{k}, \mathbf{k}'), \quad (10)$$

where

$$\mathbf{D}_{\sigma\sigma'}(\mathbf{k}, \mathbf{k}') = \psi_{\zeta,\sigma}^+(\mathbf{k}) \psi_{\zeta,\sigma'}(\mathbf{k}') \frac{1}{S} \int \mathbf{r} e^{\frac{i}{\hbar}(\mathbf{k}' - \mathbf{k})\mathbf{r}} d\mathbf{r}. \quad (11)$$

we obtained an analytical expression, which we do not explicitly present here due to its long form. In contrast to the nonrelativistic case, we found that the dipole matrix element for the light interaction with the bilayer depends on the electron momentum.

We use Heisenberg picture, where operator evolution is given by the following equation

$$i\hbar \frac{\partial \hat{L}}{\partial t} = [\hat{L}, \hat{H}], \quad (12)$$

The single-particle density matrix in momentum space is defined as:

$$\rho_{\sigma_1\sigma_2}(\mathbf{k}_1, \mathbf{k}_2, t) = \langle \hat{a}_{\mathbf{k}_2, \sigma_2}^\dagger(t) \hat{a}_{\mathbf{k}_1, \sigma_1}(t) \rangle. \quad (13)$$

Using equations Eqs.(9)-(13) one can arrive at the evolution equation for the single-particle density matrix for different values of \mathbf{k} and in external laser field:

$$i\hbar \frac{\partial \rho_{1-1}(\mathbf{k}, t)}{\partial t} = 2\mathcal{E}_{\mathbf{k}1}\rho_{1-1}(\mathbf{k}, t) + E(t) d(\mathbf{k}) [\rho_{11}(\mathbf{k}, t) - \rho_{-1-1}(\mathbf{k}, t)], \quad (14)$$

$$i\hbar \frac{\partial \rho_{11}(\mathbf{k}, t)}{\partial t} = [\rho_{1-1}(\mathbf{k}, t)(E(t)d(\mathbf{k}))^* - c.c.], \quad (15)$$

where the index ($\sigma = 1$) is connected with the conduction band and the index ($\sigma = -1$) is associated with the valence band, ρ_{11} and ρ_{-1-1} are the populations in the conduction and valence bands correspondingly, while ρ_{1-1} describes the interband polarisation induced by the laser field.

III. MANY-BODY CORRELATIONS IN BILAYER GRAPHENE

The Hamiltonian for bilayer graphene in the second quantization formalism, in the presence of electron-electron interaction, has the form

$$H = \int \Psi^\dagger H_s \Psi d\mathbf{r} + H_{Coul}, \quad (16)$$

$$H_{Coul} = \int \int \Psi^\dagger(\mathbf{r}) \Psi^\dagger(\mathbf{r}') V(|\mathbf{r} - \mathbf{r}'|) \Psi(\mathbf{r}') \Psi(\mathbf{r}) d\mathbf{r}' d\mathbf{r}. \quad (17)$$

In Eq. (16) the Hamiltonian H_s for bilayer graphene in the presence of laser field is given by Eq.(2) and \hat{H}_{Coul} is the Coulomb Hamiltonian.

Using the expansion of the fermionic field operator over the annihilation and creation operators Eq.(5), we obtain the expression for total Coulomb Hamiltonian, that consists of the four terms: $H_{Coul} = H_I + H_{II} + H_{III} + H_{IV}$.

Due to its complexity, we bring here the expression only for the first term:

$$\begin{aligned}
H_I = & \frac{1}{2} \sum_{\mathbf{k}'\mathbf{k}''\mathbf{q}} V_{2D}(\mathbf{q}) \{ \\
& \hat{c}_{\mathbf{k}'-\mathbf{q}}^+ \hat{c}_{\mathbf{k}''+\mathbf{q}}^+ \hat{c}_{\mathbf{k}''} \hat{c}_{\mathbf{k}'} f^+(\mathbf{k}' - \mathbf{q}) f^+(\mathbf{k}'' + \mathbf{q}) f(\mathbf{k}'') f(\mathbf{k}') \\
& + \hat{c}_{\mathbf{k}'-\mathbf{q}}^+ \hat{c}_{\mathbf{k}''+\mathbf{q}}^+ \hat{c}_{\mathbf{k}''} \hat{v}_{\mathbf{k}'} f^+(\mathbf{k}' - \mathbf{q}) f^+(\mathbf{k}'' + \mathbf{q}) f(\mathbf{k}'') f_v(\mathbf{k}') \\
& + \hat{c}_{\mathbf{k}'-\mathbf{q}}^+ \hat{c}_{\mathbf{k}''+\mathbf{q}}^+ \hat{v}_{\mathbf{k}''} \hat{c}_{\mathbf{k}'} f^+(\mathbf{k}' - \mathbf{q}) f^+(\mathbf{k}'' + \mathbf{q}) f_v(\mathbf{k}'') f(\mathbf{k}') \\
& + \hat{c}_{\mathbf{k}'-\mathbf{q}}^+ \hat{c}_{\mathbf{k}''+\mathbf{q}}^+ \hat{v}_{\mathbf{k}''} \hat{v}_{\mathbf{k}'} f^+(\mathbf{k}' - \mathbf{q}) f^+(\mathbf{k}'' + \mathbf{q}) f_v(\mathbf{k}'') f_v(\mathbf{k}') \}
\end{aligned}$$

Here we define the creation operator $\hat{a}_{\mathbf{k},\sigma}^+$ in the conduction band as $\hat{c}_{\mathbf{k}}^+(t)$, and annihilation operator $\hat{a}_{\mathbf{k},\sigma}$ in the valence band as $\hat{v}_{\mathbf{k}}(t)$ and $f(k)$ is the wave function Eq.(7) in the specific \mathbf{k} point.

As we see, the first Coulomb Hamiltonian H_I , by itself, consists of four terms: $H_I = H_I^1 + H_I^2 + H_I^3 + H_I^4$, and the total H_{Coul} consists of 16 terms.

The second term of Coulomb Hamiltonian H_{II} can be obtained from H_I by changing in the second column the operator related to the conduction band $\hat{c}_{\mathbf{k}''+\mathbf{q}}^+$ by the valence one $\hat{v}_{\mathbf{k}''+\mathbf{q}}^+$. These operators satisfy the anticommutation rules: $[\hat{c}_{\mathbf{k}}^+, \hat{c}_{\mathbf{k}'}]_+ = \delta_{\mathbf{k},\mathbf{k}'}$, $[\hat{c}_{\mathbf{k}}, \hat{c}_{\mathbf{k}'}]_+ = 0$, $[\hat{c}_{\mathbf{k}}^+, \hat{v}_{\mathbf{k}'}]_+ = 0$.

To take into account the contribution of the Coulomb interaction for an operator evolution in Eq.(12), we use now the total Hamiltonian given by Eq.(16).

The product of four field operators describes all many particle correlations as trions, biexcitons, etc. To take into account only excitonic effects, we apply the Hartree-Fock approximation to the many particle system, i.e. we express four field operator averages in Coulomb Hamiltonian as products of the polarization and population, e.g. for $\langle \hat{v}_{\mathbf{k}}^+ \hat{c}_{\mathbf{k}'+\mathbf{q}} \hat{c}_{\mathbf{k}+\mathbf{q}} \hat{c}_{\mathbf{k}'} \rangle$ we have

$$\langle \hat{v}_{\mathbf{k}}^+ \hat{c}_{\mathbf{k}'+\mathbf{q}} \hat{c}_{\mathbf{k}+\mathbf{q}} \hat{c}_{\mathbf{k}'} \rangle = \langle \hat{v}_{\mathbf{k}}^+ \hat{c}_{\mathbf{k}'} \rangle \langle \hat{c}_{\mathbf{k}'+\mathbf{q}}^+ \hat{c}_{\mathbf{k}+\mathbf{q}} \rangle \delta_{\mathbf{k},\mathbf{k}'} - \langle \hat{v}_{\mathbf{k}}^+ \hat{c}_{\mathbf{k}+\mathbf{q}} \rangle \langle \hat{c}_{\mathbf{k}'+\mathbf{q}}^+ \hat{c}_{\mathbf{k}'} \rangle \delta_{\mathbf{k},\mathbf{k}+\mathbf{q}} \quad (18)$$

Using this approximation, we truncate the infinite Bogolubov chain, and obtain closed set of equations which leads to exact exciton energy. Using Eqs. (9)-(18) we arrive at the evolution equations for the single-particle density matrix for different values of k_x, k_y and in the field of external laser, namely

$$i\hbar \frac{\partial \rho_{1-1}(\mathbf{k}, t)}{\partial t} = \Sigma(\mathbf{k}) \rho_{1-1}(\mathbf{k}, t) + \Lambda(\mathbf{k}) [2\rho_{11}(\mathbf{k}, t) - 1], \quad (19)$$

$$i\hbar \frac{\partial \rho_{11}(\mathbf{k}, t)}{\partial t} = [\rho_{1-1}(\mathbf{k}, t) \Lambda(\mathbf{k})^* - \rho_{-11}(\mathbf{k}, t) \Lambda(\mathbf{k})], \quad (20)$$

where

$$\Sigma(\mathbf{k}) = 2\mathcal{E}_{\mathbf{k}1} + \sum_{\mathbf{q} \neq 0} V_{2D}(\mathbf{q}) T(\mathcal{E}_{\mathbf{k}1}, U, \rho_{1-1}(\mathbf{k}), \rho_{11}(\mathbf{k})), \quad (21)$$

$$\Lambda(\mathbf{k}) = E(t)d(\mathbf{k}) + \sum_{\mathbf{q} \neq 0} V_{2D}(\mathbf{q}) P(\mathcal{E}_{\mathbf{k}1}, U, \rho_{1-1}(\mathbf{k}), \rho_{11}(\mathbf{k})). \quad (22)$$

We do not show here the obtained analytical expressions for the functions T and P because of their complicated forms. Notice, that for graphene systems the functions T and P depend on the value of the opened gap as well as on the energy (Eq. (6)).

IV. EXCITONIC ABSORPTION IN GAPPED MONOLAYER GRAPHENE

The potential energy difference, that opens an energy gap U , can be achieved in monolayer graphene by the inversion symmetry breaking. Experimentally, it can be obtained by placing graphene onto a substrate in which the A and B atoms experience different on-site energies. As shown in Ref. [22], graphene grown epitaxially on SiC has a band gap of about 0.2 eV, owing to the graphene-substrate interaction.

Here we consider the interaction of a weak electromagnetic wave with monolayer graphene in linear regime, when energy gap is opened. We assume again that the laser pulse propagates in the perpendicular direction to graphene plane (XY) and the electric field $E(t)$ of pulse with linear polarization lies in the graphene plane. We consider only low excitation regime with a small density of electrons and holes and concentrate on the analysis of one electron-hole pair effect. We use the same method, developed for bilayer graphene and based on second quantized technique. The difference is, that the Hamiltonian of gapped graphene monolayer, in the vicinity of the K point, has now the form

$$\hat{H}_0 = \begin{pmatrix} -\frac{U}{2} & v_F \hbar (k_x - ik_y) \\ v_F \hbar (k_x + ik_y) & \frac{U}{2} \end{pmatrix}, \quad (23)$$

The following calculations do not depend on s , only the spin summation leads to an extra 2 factor in the final result for macroscopic interband polarization, that is induced by an electromagnetic wave. Using macroscopic interband polarization, we compute the optical susceptibility from which we can get the absorption coefficient.

Now, we expand the fermionic field operator (see Eq.(5)) over the free wave functions of gapped monolayer:

$$\psi_{\sigma}(\mathbf{k}) = \sqrt{\frac{\mathcal{E}_{\mathbf{k}\sigma} + U/2}{2\mathcal{E}_{\mathbf{k}\sigma}}} \begin{pmatrix} 1 \\ v_F \hbar k e^{i\vartheta}/(\mathcal{E}_{\mathbf{k}\sigma} + U/2) \end{pmatrix} \quad (24)$$

$$\psi_{\sigma}(\mathbf{k})^+ = \sqrt{\frac{\mathcal{E}_{\mathbf{k}\sigma} + U/2}{2\mathcal{E}_{\mathbf{k}\sigma}}} (1, v_F \hbar k e^{-i\vartheta}/(\mathcal{E}_{\mathbf{k}\sigma} + U/2)), \quad (25)$$

where $v_F = \sqrt{3}\gamma_0 a/2\hbar$.

The expression for energy spectrum of monolayer graphene is:

$$\mathcal{E}_{\mathbf{k}\sigma} = \sigma \sqrt{\frac{U^2}{4} + (v_F \hbar k)^2} \quad (26)$$

For the dipole matrix element $d_{\sigma\sigma'}(\mathbf{k})$ for monolayer graphene we obtained the expression:

$$d_{\sigma\sigma'}(\mathbf{k}) = \frac{e\hbar v_F}{2\mathcal{E}_{\mathbf{k}1}^2 k} (-\mathcal{E}_{\mathbf{k}1} k_y + iU k_x/2) \quad (27)$$

The diagonal elements of the density matrix Eq.(13) are populations in the valence and conduction bands, correspondingly, while non-diagonal term is the interband polarization:

$$P_{\mathbf{k}}(t) = \langle \hat{v}_{\mathbf{k}}^+(t) \hat{c}_{\mathbf{k}}(t) \rangle, \quad (28)$$

$$P_{\mathbf{k}}^*(t) = \langle \hat{c}_{\mathbf{k}}^+(t) \hat{v}_{\mathbf{k}}(t) \rangle.$$

In order to find time dependent equations for the interband polarization we use Heisenberg picture, where operator evolution, e.g. for $\hat{v}_{\mathbf{k}}^+(t)$ is given by the following equation

$$i\hbar \frac{\partial \hat{v}_{\mathbf{k}}^+(t)}{\partial t} = [\hat{v}_{\mathbf{k}}^+(t), H], \quad (29)$$

where the Hamiltonian H is given by Eq. (16).

To take into account only excitonic effects, we again apply the Hartree-Fock approximation to the many particle system. In linear regime we assume that the population in the conduction band is almost zero, while the population in the valence band is unity. In this regime we have only equation for interband polarization, and that takes into account the Coulomb interaction. Using Eqs. (16,17) and Eqs. (23)-(29) we obtain the following two equations for the real and imaginary parts of the polarization $P_{\mathbf{k}}(t) = P'_{\mathbf{k}} + iP''_{\mathbf{k}} = P'_{k\vartheta} + iP''_{k\vartheta}$

$$\begin{aligned}\hbar \frac{P'_{\mathbf{k}}(t)}{\partial t} &= 2\mathcal{E}_{\mathbf{k}1}P''_{\mathbf{k}}(t) - \text{Im}[E(t)d(\mathbf{k})] + \sum_{\mathbf{q} \neq 0} V_{2D}(\mathbf{q}) [(U \sin(\vartheta - \vartheta')/2\mathcal{E}_{\mathbf{k}1})P'_{\mathbf{k}} + \cos(\vartheta - \vartheta')P''_{\mathbf{k}}] \\ \hbar \frac{P''_{\mathbf{k}}(t)}{\partial t} &= -2\mathcal{E}_{\mathbf{k}1}P'_{\mathbf{k}}(t) + \text{Re}[E(t)d(\mathbf{k})] + \sum_{\mathbf{q} \neq 0} V_{2D}(\mathbf{q}) \left[\frac{(\gamma_0^2 k k' + U^2 \cos(\vartheta - \vartheta'))}{4\mathcal{E}_{\mathbf{k}1}\mathcal{E}_{\mathbf{k}'1}} P'_{\mathbf{k}} - \frac{U \sin(\vartheta - \vartheta')}{2\mathcal{E}_{\mathbf{k}1}} P''_{\mathbf{k}} \right],\end{aligned}\tag{30}$$

$$\tag{31}$$

where $V_{2D}(\mathbf{q})$ is the Fourier transform of two-dimensional Coulomb interaction, $d(\mathbf{k})$ is defined by Eq.(27), and the electric field of laser pulse has the following form: $E(t) = \exp(-i\omega t)\exp[(-t/\tau)^2]$ with $\tau \gg T = 2\pi/\omega$. We solve the obtained integro-differential equations numerically using Runge-Kutta method with time step $\Delta t \ll T$. As a result, we obtain the interband polarization as a function of time, and define the macroscopic polarization that includes contributions from different values of \mathbf{k} : $P(t) = \sum_{\mathbf{k}} P_{\mathbf{k}}(t)d^*(\mathbf{k}) + c.c.$

Using Fourier transform of macroscopic interband polarization, we compute the optical susceptibility, and get the absorption coefficient as the imaginary part of the optical susceptibility.

V. RESULTS AND DISCUSSION

We solve numerically differential equations Eqs.(14,15) for single-particle density matrix using Runge-Kutta method. Fig. 1 shows 2D plot for the electron distribution in the conduction band $\rho_{11} = N_c$ after the interaction with the laser pulse with $\hbar\omega_0 = 8E_L$ as a function of dimensionless momentum components (in units of the Lifshitz energy $E_L = mv_L^2/2 = 1meV$ and momentum $p_L = mv_L$). Fig. 2 shows the electron distribution function $\rho_{11} = N_c$ in the conduction band for $\hbar\omega_0 = 50E_L$.

We see that for larger value of the frequency, the light grey triangle that corresponds to higher values of N_c , becomes larger, and consequently a larger number of electrons is transferred to the conduction band. It is connected with the fact, that for larger value of the frequency, the resonant value of the gap is larger: for such values of the gap, the bands in bilayer near the K point have stronger flatness. Estimations show that the density of electrons in the triangle is about $10^{11}cm^{-2}$. The high density of excitons can lead to Bose condensation phenomenon.

In contrast with this, for small values of the gap the electron transitions from the valence to the conduction band take place only from separate regions of momentum space (see Fig. 1). This is due to the fact that for low energies, close to the Lifshitz energy E_L , the isoenergetic line is dropped into four separate pockets [2, 13]. There is one central part with $p = 0$ and three "leg" pockets with $p = p_0$, so the isoenergetic line is stretched in three directions (for valley K the line is deformed along the directions $\varphi_0 = 0, 2/3\pi$ and $4/3\pi$). For small photon energies, i.e. in the case, when $\hbar\omega_0 = 8E_L$, when the resonance takes place, the influence of this effect is more observable (see small light regions on the triangle in Fig. 1).

The obtained 2D plot for the evolution of particle distribution function in the conduction band $\rho_{cc}(\mathbf{p}, \mathbf{p}, t) = \langle \hat{c}_{\mathbf{k}}^+(t) \hat{c}_{\mathbf{k}}(t) \rangle = N_c(p)$ with time is shown in Fig. 3 for the pulse having $\hbar\omega_0 = 32E_L$ with ω_0 its frequency (in units of E_L and p_L). For this case, during the interaction time $t_f = 100T$, the energy gap of bilayer graphene reaches its maximal final value $U_{fin} = 28E_L$. We see that for $\hbar\omega_0 > U_{fin}$ the electrons transfer to the conduction band in the region which is higher than the bottom of the conduction band. Fig. 3 reflects the band structure of gapped bilayer graphene with trigonal shape of energy bands which takes place due to γ_3 interaction [13]. As shown in Fig. 3, in the beginning of the interaction, the population of electrons in the conduction band is negligible (that corresponds to dark contour in Fig. 3) while in the end of the interaction we observe the full inversion of the population of electrons between the valence and the conduction bands (light contour in Fig. 3).

Fig. 4 shows excitonic absorption spectrum of gated monolayer graphene with the energy gap $500meV$ as a function of detuning $\beta = (U - \hbar\omega)/E_R$ where $E_R = \mu e^4/2\hbar^2\chi^2$ is the effective Rydberg energy. We introduce the reduced effective electron-hole mass by the expression $\mu = U/4v_F^2$; the mass is simply proportional to the band gap as in a simple two-band model proposed in [23]. In contrast to the standard semiconductor case, in graphene one deals with fine structure constant, and the appearance of bound states strongly depends on the value of $\alpha = \chi e^2/\hbar v_F$ (the choice of dielectric constant strongly affects this). For $\alpha = 0.175$ (for the value of dielectric constant $\chi = 12.5$) we obtained the maximum of the excitonic peak at $4.12E_R$ (see Fig. 4).

This result is in a good agreement with the exact analytical solution for relativistic 2D hydrogen atom [24]. The expression for the ground state energy in Ref. [24] has the form

$E_c = m_e c^2 [1 + 4\alpha^2 / (1 - 4\alpha^2)]^{-1/2}$ which gives $E \approx 4.13 E_R$ for the value of $\alpha = 0.175$.

We found that the width of the peak in Fig. 4 is much larger than in nonrelativistic case.

In a future paper, and on the basis of the above developed method, we plan to show our investigation of excitonic absorption in gaped bilayer graphene.

VI. CONCLUSIONS

In the present paper the microscopic theory of a strong electromagnetic radiation interaction with multilayer graphene systems is developed. We consider one-photon resonant interaction of a laser field with bilayer graphene when an energy gap U is opened due to external gates. We found that changing the energy gap linearly with time, the electron population is transferred from the top of valence band to the bottom of conduction one after the time t_1 , when the gap comes into resonance with the electromagnetic field.

It is well known that a frequency-chirped laser pulse may produce full inversion of the populations between the ground and excited states in the two-level atom in the adiabatic following approximation [25, 26]. The population transfer in graphene systems can also be achieved by using traditional frequency chirped electromagnetic pulses, but the suggested method (i.e. adiabatic change of the energy gap) is more convenient for graphene systems, since there are technical difficulties with terahertz radiation manipulation.

In this sense, graphene devices can in turn be used for infrared and terahertz radiation detection and frequency conversion.

We also found that due to relative flatness of the bottom (top) of conduction (valence) band in multilayer graphene systems in the presence of perpendicular electric field, the density of coherently created particle-hole pairs becomes quite large, which can make Bose-Einstein condensation of electron-hole pairs possible.

We consider also excitonic states in monolayer graphene with opened energy gap. To take into account the Coulomb interaction, we use Hartree-Fock approximation that leads to a closed set of equations for the single-particle density matrix, which in turn produce our final results for the excitonic absorption in this case. A broader investigation of excitonic absorption for gated bilayer graphene is reserved for a future article currently under preparation.

Acknowledgments

The Authors thank Dr. G.F. Mkrtchian and Prof. F.M. Peeters for fruitful discussions.

- [1] K. S. Novoselov et al., Science **306**, 666 (2004).
- [2] A. H. Castro Neto et al., Rev. Mod. Phys. **81**, 109 (2009).
- [3] K. S. Novoselov, A. K. Geim, S. V. Morozov, D. Jiang, M. I. Katsnelson, I. V. Grigorieva, S. V. Dubonos, and A. A. Firsov, Nature (London) **438**, 197 (2005).
- [4] Y. Zhang, Y.-W. Tan, H. L. Stormer, and P. Kim, Nature (London) **438**, 201 (2005).
- [5] T. Ohta, A. Bostwick, T. Seyller, K. Horn, and E. Rotenberg, Science **313**, 951 (2006).
- [6] Zhang et al., Nature (London) **459**, 820 (2009).
- [7] Li et al., Nat. Phys. **4**, 532 (2008).
- [8] A. K. Geim and K. S. Novoselov, Nature Materials **6**, 183 (2007).
- [9] P. Blake, P. D. Brimicombe, R. R. Nair, T. J. Booth, D. Jiang, F. Schedin, L. A. Ponomarenko, S. V. Morozov, H. F. Gleeson, E. W. Hill, A. K. Geim, and K. S. Novoselov, Nano Letters **8**, 1704 (2008).
- [10] K. L. Ishikawa, Phys. Rev. B. **82**, 201402(R) (2010).
- [11] M. I. Katsnelson, K. S. Novoselov, and A. K. Geim, Nature Phys. **2**, 620 (2006)
- [12] Eduardo V. Castro, K. S. Novoselov, S.V. Morozov, N. M. R. Peres, J. M. B. Lopes dos Santos, Johan Nilsson, F. Guinea, A. K. Geim, and A. H. Castro Neto, Phys. Rev. Lett. **99**, 216802 (2007).
- [13] A. A. Avetisyan, B. Partoens, and F. M. Peeters, Phys. Rev. B **80**, 195401 (2009)
- [14] A. A. Avetisyan, B. Partoens, and F. M. Peeters, Phys. Rev B **81**, 115432, (2010)
- [15] W. Bao et al., Nature Physics **7**, 948 (2011).
- [16] A.C. Ferrari et al Phys. Rev. Lett. **97**, 187401 (2006).
- [17] M.F. Craciun, S Russo, M. Yamamoto et al., Nature Nanotechnol. **4**, 383(2009).
- [18] K. F. Mak, J. Shan and T. F. Heinz., Phys.Rev. Lett. **104**, 176404 (2010).
- [19] N. M. R. Peres, R. M. Ribeiro, and A. H. Castro Neto, arXiv:1002.0464v2
- [20] Kin Fai Mak et al., Phys. Rev. Lett. **101**, 196405 (2008).
- [21] C.-H. Park and S. G. Louie, Nano Lett. **10**, 426 (2010).

- [22] S. Y. Zhou et al., Nature Mater. **6**, 770 (2007).
- [23] T. G. Pedersen, A-P Jauho, and K. Pedersen, Phys. Rev B **79**, 113406 (2009)
- [24] S. H. Guo, X. L. Yang, F. T. Chan et al., Phys. Rev. A **43**, 1197 (1991).
- [25] N. V. Vitanov et al., Annu. Rev. Phys. Chem., **52**, 763, (2001).
- [26] G. P. Djotyan et al., Phys. Rev. A **64**, 013408 (2001)

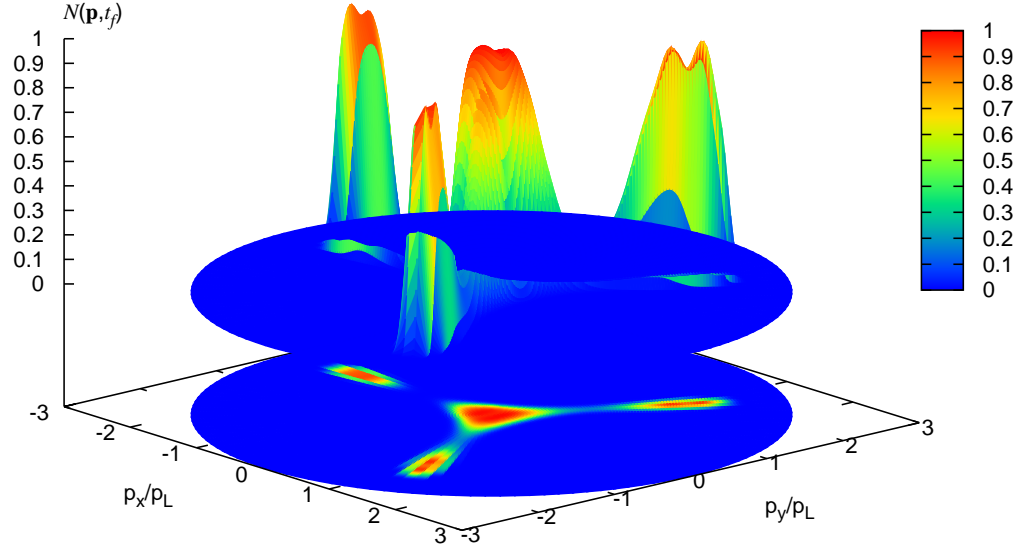


FIG. 1: Particle distribution function $N_c(p)$ (in arbitrary units) after the interaction with the pulse having $\hbar\omega_0 = 8E_L$ (when $\hbar\omega_0 \approx U_{fin}$) as a function of scaled dimensionless momentum components.

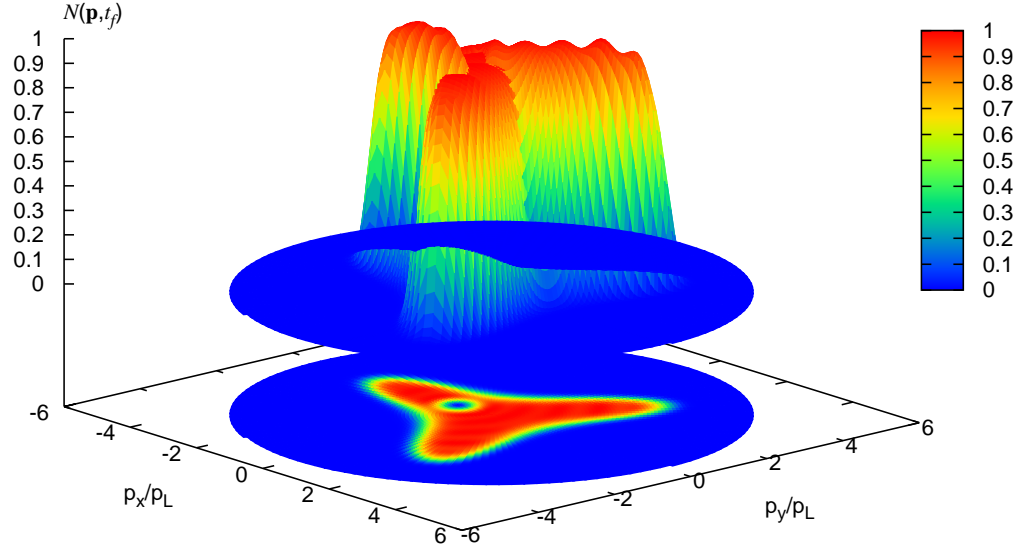


FIG. 2: Particle distribution function $N_c(p)$ (in arbitrary units) after the interaction with the pulse with $\hbar\omega_0 = 50E_L$ (when $\hbar\omega_0 \approx U_{fin}$) as a function of scaled dimensionless momentum components.

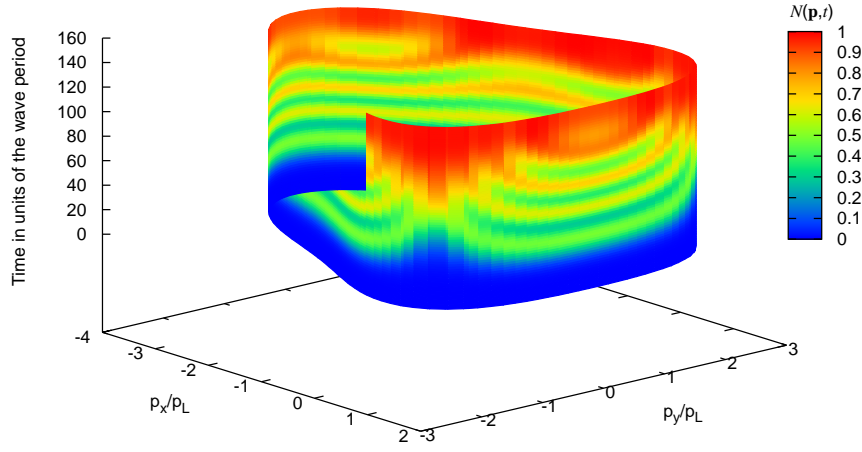


FIG. 3: The evolution of the particle distribution function $N_c(p)$ (in arbitrary units) during the interaction with the pulse with $\hbar\omega_0 = 32E_L$, when the energy gap of bilayer graphene reaches its maximal final value $U_{fin} = 28E_L$

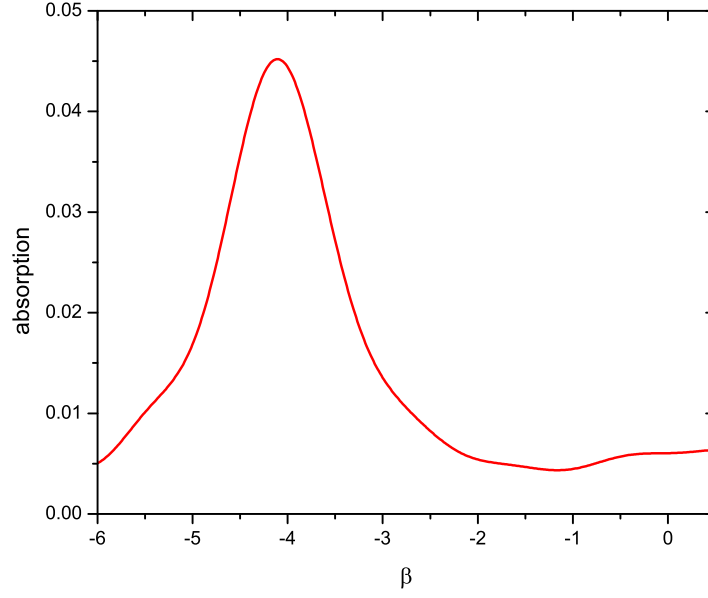


FIG. 4: Excitonic absorption in monolayer graphene as a function of the detuning $\beta = (U - \hbar\omega)/E_R$ for the value of effective fine structure $\alpha = 0.175$